Molecular Biology of the Cell
Vol. 21, 712–724, March 1, 2010

NPP-16/Nup50 Function and CDK-1 Inactivation Are Associated with Anoxia-induced Prophase Arrest in *Caenorhabditis elegans*

Vinita A. Hajeri, Brent A. Little, Mary L. Ladage, and Pamela A. Padilla

Department of Biological Sciences, University of North Texas, Denton, TX 76203

Submitted September 15, 2009; Revised December 15, 2009; Accepted December 18, 2009
Monitoring Editor: Mark J. Solomon

Oxygen, an essential nutrient, is sensed by a multiple of cellular pathways that facilitate the responses to and survival of oxygen deprivation. The *Caenorhabditis elegans* embryo exposed to severe oxygen deprivation (anoxia) enters a state of suspended animation in which cell cycle progression reversibly arrests at specific stages. The mechanisms regulating interphase, prophase, or metaphase arrest in response to anoxia are not completely understood. Characteristics of arrested prophase blastomeres and oocytes are the alignment of condensed chromosomes at the nuclear periphery and an arrest of nuclear envelope breakdown. Notably, anoxia-induced prophase arrest is suppressed in mutant embryos lacking nucleoporin NPP-16/NUP50 function, indicating that this nucleoporin plays an important role in prophase arrest in wild-type embryos. Although the inactive form of cyclin-dependent kinase (CDK-1) is detected in wild-type–arrested prophase blastomeres, the inactive state is not detected in the anoxia exposed *npp-16* mutant. Furthermore, we found that CDK-1 localizes near chromosomes in anoxia-exposed embryos. These data support the notion that NPP-16 and CDK-1 function to arrest prophase blastomeres in *C. elegans* embryos. The anoxia-induced shift of cells from an actively dividing state to an arrested state reveals a previously uncharacterized prophase checkpoint in the *C. elegans* embryo.

INTRODUCTION

Cells have adapted mechanisms to regulate or arrest cell division in response to chemical agents causing DNA damage or microtubule depolymerization. The experimental exposure of cells to these environments (e.g., UV radiation, nocodazole, benomyl) was vital for the identification and understanding of cell cycle checkpoints (Hartwell and Weinert, 1989; Nurse *et al.*, 1998). Oxygen deprivation, on the other hand, is a natural stressor that many organisms may encounter during growth and development. It was previously observed in several experimental systems, including *Caenorhabditis elegans*, *Drosophila*, zebrafish embryos, and mammalian embryonic fibroblasts in culture, that oxygen deprivation induces a reversible cell cycle arrest. Blastomeres of *C. elegans* and *Drosophila melanogaster* embryos exposed to anoxia arrest during interphase and all stages of mitosis except anaphase (Foe and Alberts, 1985; Padilla *et al.*, 2002). In *C. elegans*, this induced arrest may extend for more than 3 d in the absence of oxygen. Most remarkably, embryonic development proceeds normally after reexposure to air, and no long-term effects on the embryos can be observed; nematodes develop into adults that are morphologically indistinguishable from wild type and produce normal offspring (Padilla *et al.*, 2002). *D. melanogaster* embryos exposed to hypoxia arrest in interphase and the metaphase stage of mitosis (DiGregorio *et al.*, 2001; Douglas *et al.*, 2001). In vertebrate cells, blastomeres of zebrafish embryos exposed to anoxia arrest during interphase (S and G2 phases; Padilla and Roth, 2001) and some cultured mammalian cells exposed to hypoxia arrest in the G1 stage of the cell cycle (Green *et al.*, 2001). In all of the determined cases, the arrested cells resume cell cycle progression upon reexposure to air (normoxia). Intriguingly, anoxia-induced suspended animation and embryonic cell cycle arrest occur in such a tightly controlled manner that the arrest is maintained for several days, yet the precise specification of the diverse cell types is not lost. That is, anoxia-induced arrest of embryonic development does not alter the developmental trajectory of cells and tissues. The molecular basis for these defined cell cycle arrests and the control of resumption of the developmental program is poorly understood. It is unclear how a reduction in oxygen signals blastomeres at various stages of cell division to reversibly arrest at specific stages of the cell cycle. Understanding the phenomenon of anoxia-induced suspended animation thus may contribute to a better understanding of how environmental stress influences cell cycle progression and cell cycle checkpoints in developing embryos.

The size and transparency of *C. elegans* embryos make them an excellent model for observing cellular structures and cell division during development (Moore *et al.*, 1999; Oegema *et al.*, 2001). Examination of blastomeres from embryos exposed to anoxia indicates that significant alterations in response to oxygen deprivation occur within the nucleus. A cellular hallmark of anoxia-induced arrested blastomeres is the appearance of condensed chromatin that becomes associated with the nuclear periphery; this phenotype is observed in both interphase and prophase blastomeres (Hajeri *et al.*, 2005). A characteristic of metaphase blastomeres of embryos exposed to anoxia is the formation of nucleoporin aggregates surrounding the chromosomes, which suggests that the nuclear pore complex (NPC) breakdown is altered under this condition in com-

This article was published online ahead of print in *MBC in Press* (http://www.molbiolcell.org/cgi/doi/10.1091/mbc.E09–09–0787) on January 6, 2010.

Address correspondence to: Pamela A. Padilla (ppadilla@unt.edu).

parison to untreated embryos at a similar stage of the cell cycle (Hajeri *et al.*, 2005). Whether chromatin association with the nuclear periphery and nucleoporin aggregation are essential components of anoxia-induced cell cycle arrest is currently unknown.

Cell cycle progression is controlled by various checkpoints, and evidence from *C. elegans* and *D. melanogaster* suggests that anoxia/hypoxia specifically triggers the spindle checkpoint to maintain metaphase arrest. In yeast, mutations in the spindle checkpoint genes lead to sensitivity to microtubule-depolymerizing agents, resulting in a failure to arrest in metaphase in response to spindle damage (Hardwick *et al.*, 1999), and mutations in the essential spindle checkpoint genes in mammals may be associated with colorectal and brain tumors (Cahill *et al.*, 1998; Reis *et al.*, 2001). Exposure to anoxia or microtubule-depolymerizing agents in *C. elegans* or *D. melanogaster* embryos deficient for spindle checkpoint function leads to the inability to arrest at metaphase and a chromosome segregation phenotype (Nystul *et al.*, 2003; Fischer *et al.*, 2004; Encalada *et al.*, 2005; Pandey *et al.*, 2007; Hajeri *et al.*, 2008). Furthermore, *C. elegans* wild-type embryos exposed to anoxia contain metaphase blastomeres with a reduction in spindle and astral microtubules (Hajeri *et al.*, 2005). Experiments in *Drosophila* show that the process of chromosome attachment to the mitotic spindle might be sensitive to oxygen deprivation, suggesting that the spindle checkpoint is activated by free kinetochores (Pandey *et al.*, 2007). Together, these findings are significant because they document that the spindle checkpoint genes are activated in response to the stress of oxygen deprivation in the embryo and that this process is conserved between *C. elegans* and *Drosophila*.

Although anoxia-induced metaphase arrest triggered by the spindle checkpoint function is now well established in *C. elegans*, a different mechanism and checkpoint are responsible for anoxia-induced prophase arrest. Interestingly, the majority of arrested mitotic blastomeres are in either prophase or metaphase, and there are approximately an equal number of arrested prophase blastomeres as there are arrested metaphase blastomeres suggesting that proper arrest of a prophase blastomere is equally as important as arrest of a metaphase blastomere (Padilla *et al.*, 2002). The occurrence of different arrest scenarios suggests a dependence upon the blastomeres' position in the cell cycle at the time of exposure to anoxia and the execution by different molecular mechanisms. To begin to understand prophase arrest induced by anoxia, we considered the regulation of cellular events required for the prophase-to-prometaphase transition. Nuclear envelope breakdown (NEBD) is a significant cellular event required for the progression from prophase to prometaphase and a final commitment to mitotic progression (Margalit *et al.*, 2005; Anderson and Hetzer, 2008). To monitor cell cycle progression under normoxia and anoxia conditions, we conducted live cell imaging and found that an early response to anoxia is chromosome association with the inner nuclear membrane and inhibition of NEBD. The phenomenon of chromosome association with the nuclear periphery was also observed in oocytes of hermaphrodites exposed to anoxia as well as oocytes that are in a quiescent state due to sperm depletion (aged hermaphrodites) or disruption of fertilization (*fog-2* mutants). Using RNA interference (RNAi) and genetic mutant analysis, we determined that *npp-16*, a nonessential component of the NPC, is required for anoxia-induced prophase arrest. Furthermore, we found that in arrested prophase blastomeres of control embryos the inactive state of cyclin dependent kinase (CDK-1) is present, whereas the inactive state of CDK-1 was not detected in arrested prophase blastomeres of the *npp-16* mutant embryo. These data support the idea that NPP-16 and CDK-1 function in concert to arrest prophase blastomeres in response to anoxia. Given that oxygen deprivation plays a central role in resistance of solid tumor cells to radiation and chemotherapy treatments, these studies provide novel evidence of how oxygen deprivation influences cell division and reveal mechanistic insight into a poorly understood cell cycle arrest position during mitosis–late prophase arrest.

MATERIALS AND METHODS

Strains and Growth Conditions

The *C. elegans* wild-type N2 Bristol strain was raised on NGM plates seeded with *Escherichia coli* (OP50) as previously described (Sulston, 1988). For all experiments the nematodes were maintained at 20°C. The following strains were obtained from *Caenorhabditis elegans* Genetics Center and raised under similar conditions as the wild-type strain: TH32 (*tbg-1::GFP; pie-1::GFP::H2B*), RB1534 (*npp-16(ok1839)*), CB4108 (*fog-2(q71)*). For some assays the *BN68* strain (*pie-1::GFP::npp-5; pie-1::mCherry::his-58*), obtained from the Askjaer lab (CABD, CSIC–Universidad Pablo de Olavide, Sevilla, Spain), was used to monitor NEBD (Rodenas et al., 2009). The *Caenorhabditis elegans* Gene Knockout Consortium (Oklahoma Medical Research Foundation) produced the *npp-16(ok1839)* deletion allele (strain RB1534), which has a 1120-base pair deletion resulting in removal of amino acids 175-472 of the 512-amino acid nucleoporin NPP-16 protein. The *npp-16(ok1839)* was backcrossed three times to wild-type N2 animals to produce the strain PM118 in which all analyses were conducted. Using standard genetic techniques, the TH32 strain was crossed with the *npp-16(ok1839)* deletion PM118 strain to produce strain PM119 (*npp-16(ok1839); tbg-1::GFP; pie-1::GFP::H2B*) or the *CB4108* strain to produce *PM122* (*fog-2(q71); tbg-1::GFP; pie-1::GFP::H2B*). The genotype of *npp-16(ok1839)* allele was verified by conducting single worm PCR using *npp-16* forward primer (5′-TGACTCATCGAGCCTGAAAA-3′) and *npp-16* reverse primer (5′-GAGTCGAACTTCCCAAGCAG-3′).

Live Animal Imaging Analysis

Live animal imaging analysis was conducted using strains TH32 (*tbg-1::GFP; pie-1::GFP::H2B*) and PM119 (*npp-16(ok1839); tbg-1::GFP; pie-1::GFP::H2B*), which are both expressing γ-tubulin::GFP and histone2B::GFP, as previously described (Hajeri *et al.*, 2008). These strains allow one to monitor mitotic progression by visualization of centriole location and chromosome condensation based on green fluorescent protein (GFP) fluorescence detection. Nematodes were grown to adulthood on NGM plates seeded with *E. coli*. Gravid adults were anesthetized (0.5% tricaine, 0.05% tetramisole [Sigma-Aldrich, St. Louis, MO] in M9 buffer) and mounted on 2% agarose pads placed on coverslips (Warner Instruments, Hamden, CT); this method to anesthetize adults slows their movement during microscopic examinations, but does not interfere with ovulation and fertilization. The anesthetized nematodes were coated with a drop of halocarbon oil to prevent desiccation during exposure to a flow of nitrogen gas or air and placed in an enclosed chamber (Harvard Apparatus, South Natick, MA; Leiden closed perfusion microincubator). To monitor anoxia-induced prophase arrest, the chamber was perfused with 100% nitrogen (Air Liquide-Calgaz, Cambridge, MD), and time-lapse images of embryos within the uterus of the adult nematode were collected using a spinning disk confocal microscope (McBain Systems, Simi Valley, CA; see below). To document recovery of arrested prophase blastomeres, the nitrogen flow to the perfusion chamber was discontinued, and embryos were allowed to recover in air and imaged using time-lapse microscopy. The integrated Simple PCI software program (Hamamatsu, Bridgewater, NJ) was used for image analysis and to assess the statistics of anoxia-induced prophase arrest and recovery. To analyze mitotic progression in animals exposed to normoxia conditions, a similar methodology was followed without the nitrogen flow through the chamber. The time-lapsed movies were processed by using ImageJ (NIH; http://rsb.info.nih.gov/ij/) and imported into QuickTime (Apple Computer, Cupertino, CA) for display.

Analysis of Bivalent Prophase Chromosomes in Oocytes

To analyze the nuclear location and movement of bivalent chromosomes in oocytes of animals exposed to stress (anoxia, starvation, sodium azide) or animals with quiescent oocytes (aged animals, *fog-2* mutant), time-lapse microscopy of the primary oocytes of *TH32* animals (*tbg-1::GFP; pie-1::GFP::H2B*) *and PM122* (*fog-2(q71); tbg-1::GFP; pie-1::GFP::H2B*) animals was conducted. For anoxia assays, 1-d-old TH32 adults were exposed to 24 h of anoxia using the anaerobic bio-bag type A environmental chamber as previously described (Padilla *et al.*, 2002). After anoxia exposure, animals were quickly mounted on a 2% agar pad, and time-lapse microscopy of oocytes was conducted; all image acquisition was performed within 10 min of reexposure to normoxia. Control oocytes were from 1-d-old TH32 animals exposed to a normoxic environment. For analysis of oocytes from starved animals, 1-d-old hermaphrodites were washed four times in M9 buffer to remove *E. coli* and then placed

on an unseeded NGM plate for 12 h. These starved adults held embryos within the uterus, indicating that the lack of food was indeed inducing a physiological response. To analyze oocytes of 1-d-old hermaphrodites with blocked respiratory function, animals were placed in M9 buffer with 10 mM sodium azide for up to 1 h. Quiescent oocytes were analyzed from aged TH32 animals (6 d after L4 molt) and 1-d-old PM122 (*fog-2(q71), pie-1::GFP::H2B*) animals. For all assays, time-lapse microscopy of primary oocytes was conducted, to examine the localization and movement of bivalent prophase chromosomes within the nucleus, using a spinning disk confocal microscope (McBain Systems) and processed using ImageJ software (NIH) and Adobe Photoshop (San Jose, CA).

Indirect Immunofluorescence Assays

For indirect immunofluorescence assays embryos from young adults were collected and processed as previously described (Hajeri *et al.*, 2005); with the exception of anti-CDK-1 the method used is as described in Boxem *et al.* (1999). The following primary antibodies were used: anti-Phos H3 to detect the phosphorylated (Ser10) form of Histone H3 (Upstate Biotechnology, Lake Placid, NY); mAb414 to detect the nuclear pore complex (Babco, Berkeley, CA); anti-HCP-3 to detect the centromeric histone HCP-3 (Buchwitz *et al.*, 1999); YL1/2 antibody to detect microtubules (Amersham Life Science, Little Chalfont, Buckinghamshire, England); and anti-CDK-1$^{P\text{-}Tyr15}$ antibody to detect the inactive form of CDK-1 (Calbiochem, San Diego, CA; Hachet *et al.*, 2007) and a polyclonal antibody raised against the C terminus of CDK-1 (a kind gift from A. Golden [National Institute of Diabetes and Digestive and Kidney Diseases, Bethesda, MD] and J. Schumacher [University of Texas M.D. Anderson Cancer Center, Houston, TX]; Boxem *et al.*, 1999). All primary antibodies were used in a working dilution of 1:500, except anti-CDK-1$^{P\text{-}Tyr15}$ was used in a working dilution of 1:100 and anti-CDK-1 was a 1:1000 working dilution. Embryos were examined using a Zeiss Axioscope fluorescence microscope (Thornwood, NY). Embryos were examined and images obtained using a spinning disk confocal microscope (McBain Systems) at a consistent temperature of 22°C. Specifications for the confocal microscope were as follows: Zeiss 200M microscope with Apochromat 40×, LCI Plan Neofluar 63×, or Plan Apochromat, 100× objectives, and images were acquired with a Hamamatsu Electron Multiplier CCD camera (model C9100-02). Image acquisition software was Simple PCI (Hamamatsu) and images were processed using ImageJ software (NIH) and Adobe Photoshop (Hajeri *et al.*, 2005).

Analysis of the germline was conducted in a similar manner as previously described (Jud *et al.*, 2008). Briefly, 1-d-old hermaphrodites were transferred to M9 and washed twice to remove bacteria. Approximately 20 animals were placed on a coverslip and gonads were extruded using a 27-gauge syringe needle, fixed for 20 min in 2% paraformaldehyde in a humid chamber, placed on a poly-lysine–coated slide, freeze-cracked, and fixed in −20°C methanol for 10 min. Slides were incubated with mAb414 for 1 h and secondary antibody for 30 min at room temperature. To stain DNA, DAPI was included in the last rinse before mounting for microscopy analysis. The dissected gonads were examined using both a Zeiss Axioscope fluorescence microscope or a spinning disk confocal microscope (McBain Systems); image acquisition was done using Simple PCI (Hamamatsu) and processed using ImageJ software (NIH) and Adobe Photoshop (Hajeri *et al.*, 2005).

Nocodazole Assays

To determine if microtubule depolymerization induced prophase arrest and prevented NEBD, the TH32, BN68, or N2 embryos were treated with the microtubule-depolymerizing drug nocodazole (Sigma-Aldrich) as previously described (Moore et al., 1999; Nystul et al., 2003). Gravid adults were dissected in M9 buffer to release embryos and exposed for 5 min to nocodazole (0.2 mg/ml final concentration) or M9 for controls. Embryos were collected by mouth pipetting, mounted on 2% agar pads, and covered with a coverslip; slight pressure on the coverslip was placed to ensure nocodazole entry into the embryo. Time-lapse microscopy using a spinning disk confocal microscope was conducted with the TH32 or BN68 embryos. Indirect immunofluorescence assays were performed with fixed N2 embryos to assay efficiency of microtubule depolymerization by nocodazole treatment.

Sodium Azide Assays

For analysis of embryos exposed to the respiratory chain inhibitor, sodium azide, embryos were dissected from gravid adults and placed in M9 buffer or M9 buffer containing sodium azide (10 mM) (Sigma-Aldrich) for 30 or 60 min. After sodium azide treatment, embryos were frozen on dry ice, fixed, and stained with DAPI, Phos-H3, and mAb414 antibodies. Image acquisition and analysis was done as described above. To determine the viability of embryos exposed to sodium azide, embryos were collected after treatment, washed three times in M9 buffer, and then placed on an NGM plate seeded with *E. coli*. The embryos were maintained at 20°C and assayed for their ability to hatch after 24 h. Three independent assays, with a total of at least 200 embryos, were conducted. Data were evaluated using Student's *t* test to determine p values.

RNAi Screen of Nucleoporin Genes

A synchronous population of TH32 (*tbg-1::GFP; pie-1::GFP::H2B*) L1 larvae were grown to adulthood on RNAi plates (NGM supplemented with 200 μg/ml ampicillin, 12.5 μg/ml tetracycline, and 2 mM IPTG). The RNAi plates were seeded with the *E. coli* strain for RNAi of a specified gene of interest. The *E. coli* strains were developed by the J. Ahringer laboratory and obtained from the Medical Research Council Geneservice (Cambridge, United Kingdom; Kamath *et al.*, 2003). As a control, worms were fed the *E. coli* HT115 strain containing the plasmid L4440 without insert. Adult RNAi-treated animals, which did not show a phenotype under normoxic conditions (*npp-14(RNAi), npp-16(RNAi)* and *npp-18(RNAi)*) were exposed to 24 h of anoxia using the anaerobic bio-bag Type A environmental chamber (Fisher Scientific [Pittsburgh, PA]; Padilla *et al.*, 2002; Hajeri *et al.*, 2008). After anoxia exposure, the adults were quickly transferred to a 2% agar pad and assayed for the presence of prophase-arrested blastomeres and abnormal nuclei by spinning disk confocal microscopy. To determine if RNAi of *npp-14*, *npp-16*, or *npp-18* affected mitotic progression in normoxic embryos, gravid adults were anesthetized (0.5% tricaine, 0.05% tetramisole in M9) and mounted on 2% agarose pads, and live cell imaging of the embryos in the uterus was performed. Anoxia viability assays for embryos were conducted as previously described (Padilla *et al.*, 2002; Nystul *et al.*, 2003). Young adults were dissected, and two-cell embryos were collected, placed on NMG plates, and exposed to either normoxic or anoxic environments (anaerobic bio-bag Type A environmental chamber) for 24 h. On reexposure to oxygen, the embryos were given 24 h to recover, and survivors were quantified.

Fluorescently Labeled Dextran Assays

To determine the nuclear permeability of embryos under normoxic and anoxic conditions, the TH32 (*tbg-1::GFP; pie-1::GFP::H2B*) and PM119 (*npp-16(ok1839); tbg-1::GFP; pie-1::GFP::H2B*) animals were injected in one syncytial gonad arm with either 10-, 40-, or 70-kDa dextran coupled to tetramethylrhodmine (TMR) isothiocyanate (Sigma-Aldrich) as described by Galy *et al.* (2003). The TMR-dextran molecule was diluted to a final concentration of 2 mg/ml in injection buffer (20 mM KPO_4, pH 7.5, 3 mM K citrate, 2% polyethylene glycol-6000). Injected worms were incubated for 4 h at 23 or 20°C to allow incorporation of the dextran into newly formed embryos. Adult animals were either directly dissected for imaging of the normoxic embryos or exposed to 24 h of anoxia before dissection, using the anaerobic bio-bag Type A environmental chamber, as previously described (Padilla *et al.*, 2002). Nuclear permeability was evaluated by assaying the exclusion or inclusion of fluorescently labeled dextran within the nucleus. The TH32 strain with GFP-labeled chromosomes and centrioles was used to identify mitotic cells. Embryos were analyzed, and images were collected using a Zeiss Mot II Plus microscope, Axiocam camera, and software.

RESULTS

Chromosomes Associate with the Nuclear Periphery in Anoxia-arrested Prophase Cells

Blastomeres of *C. elegans* embryos exposed to anoxia arrest during interphase and specific stages of mitosis (primarily metaphase and prophase and not anaphase; Foe and Alberts, 1985; Padilla *et al.*, 2002). Previously we have shown that arrested prophase blastomeres of embryos exposed to anoxia have fully condensed chromosomes that align at the nuclear periphery (Hajeri *et al.*, 2005). To further characterize prophase chromosome alignment with the nuclear periphery and prophase arrest, we conducted live-cell imaging analysis using a *C. elegans* strain expressing γ-tubulin::GFP and histone2B::GFP fusion proteins (*tbg-1::GFP*; *pie-1::GFP::H2B*). This strain, referred to as TH32, was used throughout our study to follow chromosome location within the nucleus and cell cycle progression. Embryos, within the uterus of gravid adult animals placed in a gas flow-through chamber, were visualized using a spinning disk confocal microscope. The animals were exposed to either air (normoxia) or nitrogen gas (anoxia). We found that the condensed chromosomes aligned at the nuclear periphery in prophase blastomeres exposed to anoxia for 8.5 min, demonstrating the fast response to anoxia conditions. Furthermore, the round nucleus morphology was maintained suggesting an arrest of NEBD (Figure 1A, Video 1). On reexposure to air, within ~4 s, the chromosomes move off the nuclear envelope, and the arrested prophase blastomere progresses through mitosis, as evidenced by the observation of NEBD and formation of the metaphase plate (Video 2). We observed that the longer the exposure time to anoxia (24 h anoxia), the longer (>15 min) it took for the chromosomes aligned with the inner nuclear

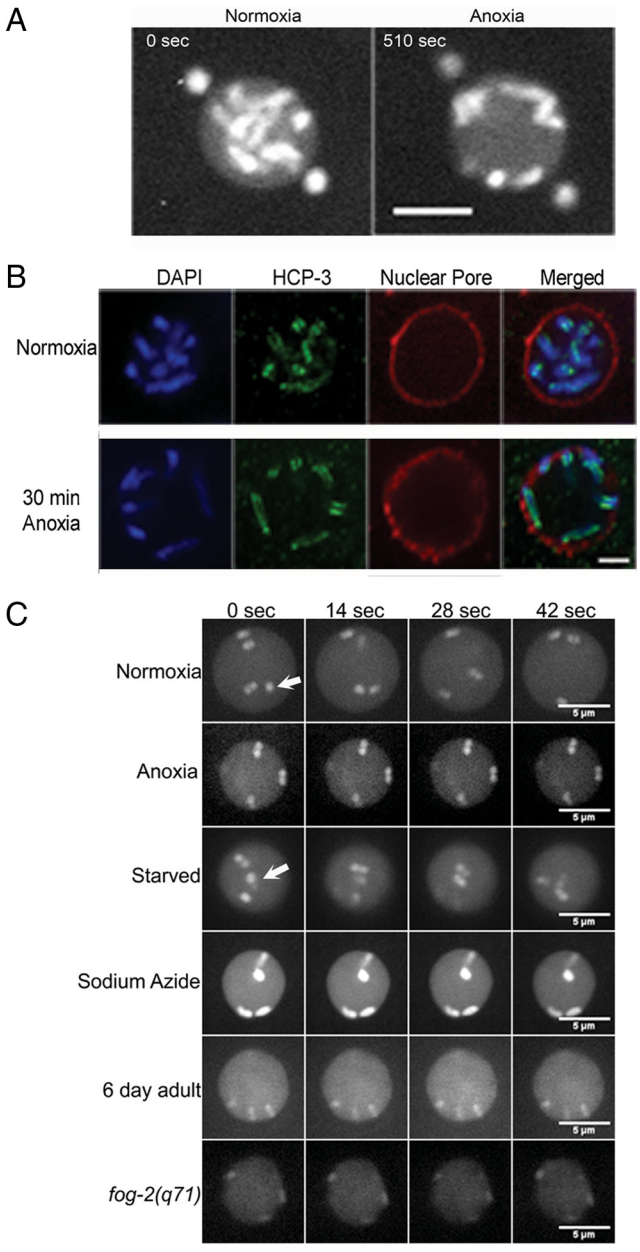

Figure 1. Chromosomes associate with the nuclear periphery in anoxia-arrested prophase blastomeres and quiescent oocytes. (A) Live cell imaging, using a *tbg-1::GFP; pie-1::GFP::H2B* strain (TH32), of embryos exposed to normoxia or anoxia (510 s) shows that the anoxia-exposed prophase blastomeres contain chromosomes that are associated with the nuclear periphery, whereas the normoxia exposed blastomeres do not. Scale bar, 5 μm. (B) Embryos exposed to either 30 min of anoxia or normoxia were stained with DAPI to detect DNA, anti-HCP-3 to detect centromeric histone, and mAb414 to recognize the NPC. Three independent experiments were conducted in which a final total of 150 prophase blastomeres from 90 embryos were examined. Scale bar, 2 μm. (C) Live cell imaging, using a *tbg-1::GFP; pie-1::GFP::H2B* strain (TH32), to analyze the chromosomes in the oocyte of adult control animals exposed to either normoxia, anoxia, starvation, or sodium azide or in a quiescent state due to sperm depletion in aged hermaphrodites or sperm dysfunction in the *fog-2(q71)* females. Time-lapse analysis was used to track chromosome location within the nucleus. Arrows point to representative chromosomes that move within the nucleus. For each experiment, at least 30 oocytes from three independent experiments were examined. Scale bar, 5 μm.

periphery to move off (data not shown). This is consistent with our previous findings that recovery from cell cycle arrest is dependent on anoxia exposure time (Hajeri *et al.*, 2005). In control prophase blastomeres of embryos exposed to normoxia, the chromosomes localized without specific arrangements and were dispersed throughout the nucleus (Figure 1A). Next, we used indirect immunofluorescence to detect the centromeric histone CENP-A/HCP-3 and NPCs and found that the centromere structure was not altered in prophase chromosomes that were associated with the nuclear periphery, further suggesting that chromosome structure remains intact in arrested prophase blastomeres (Figure 1B). The ability of anoxia-exposed embryos to maintain chromosome structure is in agreement with our previous finding that these embryos are able to recover from the arrest and progress normally through embryogenesis (Padilla *et al.*, 2002).

Because prophase cells are not only present in the embryo but also within the germline, we next investigated the impact of anoxia on the chromosome organization in oocytes. The oocytes in adult hermaphrodites are in diakinesis of prophase I and contain observable bivalent chromosomes (McCarter *et al.*, 1999). Previously, we showed that anoxia induces an arrest of oocyte maturation and ovulation in the adult hermaphrodite (Mendenhall *et al.*, 2009). We, therefore, wanted to determine if anoxia also affects bivalent chromosome location within the nucleus of oocytes. We analyzed oocytes in adults exposed to 24 h of anoxia (using the anaerobic biobags) or brief periods of anoxia using the N_2 gas flow through chamber. In control animals exposed to normoxic conditions, the bivalent chromosomes are found to move throughout the nucleoplasm of oocytes in hermaphrodites (Figure 1C). However, using the TH32 strain, we indeed found that the bivalent chromosomes aligned with the nuclear periphery in arrested oocytes of adult hermaphrodites exposed to anoxia (Figure 1C). This chromosome alignment was observed in all oocytes and not just the primary oocyte (Figure S1). Oocytes of adult animals exposed to anoxia are viable and able to be fertilized after anoxia treatment, as determined by oocyte maturation rate assays conducted in postanoxic hermaphrodites (data not shown). We did find that after longer exposures to anoxia (24 h) it took ~1.5 h for oocytes to recover in air and proceed with ovulation (n = 6). To determine how quickly the chromosomes respond to anoxia we used the N_2 gas flow-through chamber and found that chromosomes aligned with the inner nuclear periphery after exposure to 12 min of N_2 gas flow. On reexposure to normoxic conditions, the chromosomes within the primary oocyte moved off the nuclear envelope just before maturation and ovulation, whereas the chromosomes in the other oocytes remained associated with the inner nuclear periphery (n = 6 germlines observed). This suggests that the recovery process may be linked with signals involving oocyte maturation and ovulation. Furthermore, these results show that similar to prophase blastomeres, oocytes also contain chromosomes associated with the inner nuclear periphery after exposure to anoxia.

Because anoxia is a stress phenomenon that induces arrest of oocyte fertilization, we next wanted to determine if bivalent chromosome alignment with the nuclear periphery is a characteristic that is also associated with stresses and/or with quiescent oocytes. We found that starving adult hermaphrodites for 12 h, which caused adults to hold embryos in the uterus (data not shown), did not induce bivalent chromosomes to align with the nuclear periphery (Figure 1C). To test whether bivalent chromosome alignment with the nuclear periphery was induced by lack of respiratory

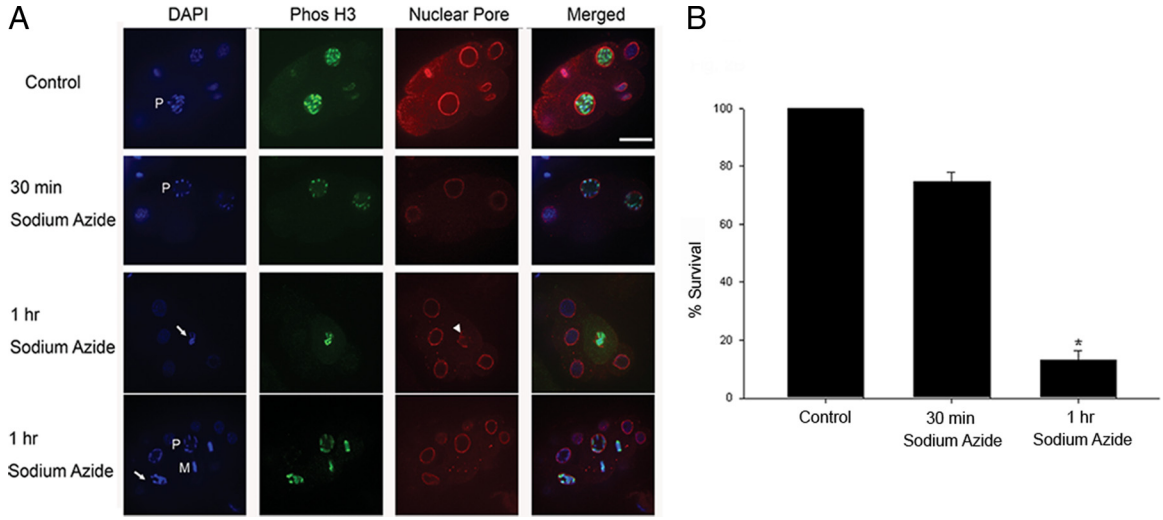

Figure 2. Inhibition of electron transport induces chromosome alignment with the nuclear periphery, nuclear abnormalities, and decreased viability. (A) Embryos exposed to sodium azide and control embryos were stained with DAPI to detect DNA, Phos H3 to detect the mitotic marker phosphorylated Histone H3, and mAb414 to detect NPC. The sodium azide–exposed embryos contain prophase blastomeres (P) with chromosomes associated with inner nuclear membrane, abnormal chromosome structure (arrow), and abnormal NPC (arrowhead). Normal metaphase blastomeres (M) were observed. Three independent experiments were conducted in which a final total of 300 mitotic blastomeres from 90 embryos were examined. Scale bar, 10 μm. (B) Embryos exposed to sodium azide, for the time indicated, washed three times in M9 buffer, and assayed for ability to develop into L1 larvae at 20°C was determined. At least 50 embryos from three independent experiments were assayed. *$p < 0.001$ in comparison to control, using Student's t test.

function, we treated animals with sodium azide, an inhibitor of cytochrome C in the electron transport chain, which is also known to induce ovulation arrest. Indeed, as shown in Figure 1C, many of the bivalent chromosomes also aligned with the nuclear periphery in animals exposed to sodium azide. This phenotype may be associated with the azide-induced ovulation arrest. We found that bivalent chromosomes also aligned with the nuclear periphery in quiescent oocytes of animals in which ovulation does not or only rarely occurs due to sperm depletion (aged hermaphrodites) or nonfunctional sperm (*fog-2(q71)* mutant; Figure 1C; Schedl and Kimble, 1988; Jud *et al.*, 2008). We did not observe any major difference in the chromosome association with the inner nuclear periphery in anoxia-arrested oocytes compared with the quiescent oocytes due to sperm depletion or dysfunction. These data suggest that bivalent chromosome association with the nuclear periphery is not signaled by stress per se but is rather a phenotype associated with stress-induced arrest or quiescence.

Anoxia and Electron Transport Inhibition Do Not Induce Identical Phenotypes

To further investigate the mechanism that regulates prophase arrest, we considered two hypotheses: 1) Prophase arrest occurs in response to a reduction in energy, or 2) prophase arrest is regulated by a genetic mechanism, such as a defined cell cycle checkpoint. The first hypothesis is based on the finding that the ATP/ADP ratio is decreased in *C. elegans* exposed to anoxia (Padilla *et al.*, 2002). The second hypothesis is based on the finding that anoxia-induced metaphase arrest requires the spindle checkpoint pathway; therefore, it is plausible to assume that prophase arrest is also controlled by a cell cycle checkpoint (Nystul *et al.*, 2003). To address the first hypothesis, we exposed embryos to sodium azide, to reduce ATP production by inhibiting electron transport activity, and examined chromosome location in prophase blastomeres and embryo viability. Indirect immunofluorescence and antibodies to detect the phosphorylated forms of histone H3 (Phos H3) or NPC (mAb414) were used to identify prophase blastomeres (Padilla *et al.*, 2002). We found that chromosomes aligned with the nuclear periphery in prophase blastomeres of embryos exposed to sodium azide for 30 or 60 min (Figure 2A), suggesting that a reduction in energy, via sodium azide exposure, is sufficient to initiate chromosome relocalization. However, in mitotic blastomeres of embryos exposed to sodium azide a dramatic increase in abnormal chromosome morphology was observed between 30- (2.38%, n = 304) and 60-min exposure to azide (24.3%; n = 239; Figure 2A, arrow). Furthermore, unlike embryos exposed to anoxia, which can survive up to 3 d in the absence of oxygen (Padilla *et al.*, 2002), the embryos exposed to 1 h of sodium azide had a significantly decreased survival rate (Figure 2B), indicating fundamentally different molecular mechanisms of cell cycle arrest.

Nucleoporin NPP-16/Nup50 Function Is Required for Prophase Arrest

To test the hypothesis that anoxia-induced prophase arrest is regulated by a genetic mechanism, such as a cell cycle checkpoint, we considered the cell cycle events that must be regulated in the arrested prophase blastomere. The transition from prophase to prometaphase is characterized by chromosome condensation, NEBD, and the initiation of chromosome movement to the equatorial plate; NEBD is considered a commitment to mitosis. The regulation of NEBD is not completely understood, but several studies show that the mechanical tension produced by microtubule polymerization may tear holes in the nuclear envelope, thus initiating NEBD (Beaudouin *et al.*, 2002; Salina *et al.*, 2002). We have previously shown that microtubules in fact depolymerize in embryos exposed to anoxia (Hajeri *et al.*, 2005). Therefore, to determine if microtubule depolymerization generates a signal for chromosomes to align with the nuclear periphery and/or arrest cells at prophase, we exposed em-

bryos to nocodazole. We tested this in three different strains (N2, TH32, and BN68) and stained for microtubules, NPC, and DNA in the N2 strain (Figure S2) or conducted live imaging analysis of the prophase blastomeres in the TH32 strain (data not shown) or BN68 strain (Videos 3 and 4). We did not observe chromosome alignment with the nuclear membrane or prophase arrest in these embryos (Figure S2, Video 4). Embryos exposed to nocodazole were affected because there was a decrease in detection of microtubules (Figure S2), and embryos contained abnormal nuclei due to DNA material outside of the nucleus (Video 4). Our findings are consistent with other reports showing that microtubule polymerization is not essential for NEBD (Encalada *et al.*, 2005; Margalit *et al.*, 2005).

It is postulated that NEBD is preceded by a stepwise disassembly of NPC and activation of specific kinases, such as cyclin-dependent kinase (CDK1), to phosphorylate proteins associated with the inner nuclear membrane (Margalit *et al.*, 2005; Galy *et al.*, 2008). The NPC in mammals is composed of about ~30 nucleoporins, several of which are known to have additional functions besides the transport of macromolecules in and out of the nucleus (D'Angelo and Hetzer, 2008). In *Drosophila* and *C. elegans* embryos and starfish oocytes the disassembly of nucleoporins occurs before the disassembly of inner nuclear membrane–associated proteins (Lee *et al.*, 2000; Kiseleva *et al.*, 2001; Lenart *et al.*, 2003). Therefore, we next tested if nucleoporin function was involved in the signaling of anoxia-induced prophase arrest. In *C. elegans* there are 24 genes predicted to encode nucleoporins (Galy *et al.*, 2003; D'Angelo and Hetzer, 2008). Using RNAi to knock down individual NPC components, we found, consistent with previous reports, that most nucleoporin genes serve essential functions and accordingly knockdown resulted in various phenotypes including embryo lethality, sterility, larval lethality, and larval arrest. However, RNAi of the nucleoporin genes *npp-14*, *npp-16*, or *npp-18* (predicted homologues of mammalian Nup214, Nup50, and Seh1, respectively) did not result in obvious phenotypes (Galy *et al.*, 2003); this allowed us to test the hypothesis that nucleoporins are involved in anoxia-induced prophase arrest. We therefore exposed *npp-14(RNAi)*, *npp-16(RNAi)*, and *npp-18(RNAi)* animals, in the TH32 strain background, to anoxia and analyzed prophase chromosome location and nuclear structure. Indeed, we found that the *npp-16(RNAi)* embryos exposed to anoxia contained blastomeres with abnormal nuclei (data not shown). These observations were confirmed and further analyzed with an *npp-16* deletion mutant, *npp-16(ok1839)*. We found that young *npp-16(ok1839)* embryos have a reduced viability when exposed to anoxia (53.1% ± 2.1), but develop almost normally in the presence of normoxia (91.6% ± 2.1); N2 control embryos survive anoxia at a rate of 100%. By using indirect immunofluorescence we observed that the *npp-16(ok1839)* embryos exposed to anoxia contain some prophase blastomeres in which the chromosomes aligned with the nuclear periphery. In addition, the embryos also contained blastomeres with abnormal nuclei, as determined by abnormal chromosome structure (Figure 3, A and B, arrow) and aggregation or abnormal distribution of NPC (Figure 3, A and B, arrowhead). These phenotypes were not observed in the *npp-16(ok1839)* embryos under normoxia conditions (Figure 3A).

To determine if the abnormal nuclei observed in anoxia exposed *npp-16(ok1839)* embryos were due to blastomeres that were unable to arrest at a specific position during mitosis, we quantified the mitotic index for young embryos. We determined that the *npp-16(ok1839)* embryos exposed to anoxia harbored a decreased number of prophase blastomeres and an increase in abnormal nuclei (Figure 4), compared with wild-type control animals under these condi-

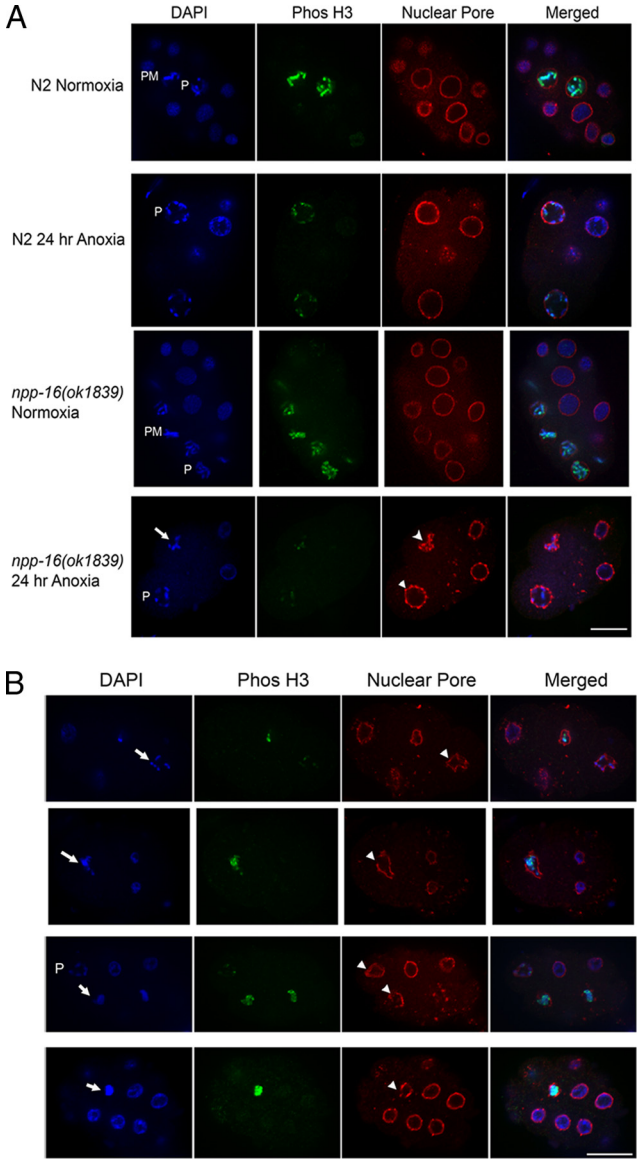

Figure 3. The *npp-16(ok1839)* embryo exposed to anoxia has an aberrant nuclear morphology. (A) N2 wild-type and *npp-16(ok1839)* embryos were stained with DAPI to detect DNA, Phos H3 to detect the mitotic marker phosphorylated Histone H3, and mAb414 to detect NPC. N2 wild-type and *npp-16(ok1839*) embryos exposed to normoxia contain normal prophase (P) and prometaphase blastomeres (PM). N2 wild-type embryos exposed to anoxia contain prophase blastomeres in which the chromosomes align with the nuclear periphery (P). The *npp-16(ok1839)* embryos exposed to anoxia contain prophase blastomeres with chromosomes that align with the nuclear periphery (P) and blastomeres with abnormal chromosome structure (arrow) or abnormal NPC structure/aggregates (arrowhead). Three independent experiments were conducted in which a final total of 250 mitotic blastomeres from 90 embryos were examined. Scale bar, 10 μm. (B) Various chromosomal abnormalities are observed in *npp-16(ok1839)* embryos exposed to anoxia. Embryos were stained with DAPI to detect DNA, Phos H3 to detect the mitotic marker phosphorylated Histone H3, and mAb414 to detect NPC. Arrow points to abnormal chromosome structure; arrowhead points toward abnormal NPC distribution. These abnormalities are associated with mitotic nuclei of embryos exposed to anoxia. Scale bar, 10 μm.

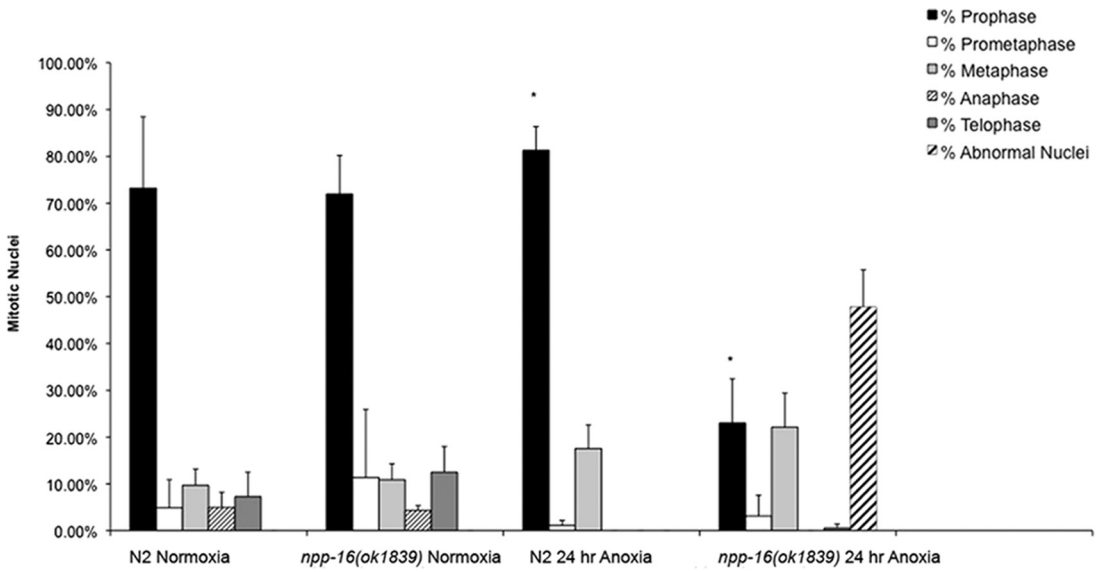

Figure 4. The mitotic index for N2 control and *npp-16(ok1839)* embryos exposed to normoxia or anoxia. The percentage of nuclei at various stages of mitosis, and the percentage of abnormal nuclei was quantified. The abnormal nuclei were positive for PhosH3 staining, indicating that these nuclei were mitotic. In comparison to N2 control embryos exposed to 24 h of anoxia, the number of prophase blastomeres significantly decreased and the number of abnormal nuclei significantly increased in *npp-16(ok1839)* embryos exposed to 24-h anoxia (*$p < 0.001$ using a Student's *t* test). Abnormal nuclei were observed in *npp-16(ok1839)* embryos exposed to 24-h anoxia. Three independent experiments were conducted in which a final total of 200 mitotic blastomeres from at least 60 embryos (2–20 cell stage) were examined.

tions. The number of metaphase blastomeres was not significantly altered between control and *npp-16(ok1839)* embryos exposed to anoxia, suggesting that *npp-16* function is specific for prophase arrest and not involved in metaphase arrest. There was no significant difference between the mitotic indices of *npp-16(ok1839)* and control embryos exposed to normoxia (Figure 4). Together, these results suggest that *npp-16* function is required for anoxia-induced prophase arrest, and that in the absence of *npp-16* function the cell cycle progresses, thus leading to abnormal nuclei.

To further determine if the presence of abnormal nuclei in *npp-16(ok1839)* embryos exposed to anoxia is due to the inability of prophase blastomeres to arrest, we conducted live cell imaging analysis in both the TH32 strain and in *npp-16(ok1839)* mutant strain, which was backcrossed into the TH32 strain (Figure 5, Videos 5 and 6). As previously described (Figure 1A), prophase blastomeres from the TH32 control strain exposed to anoxia contain chromosomes that associate with the nuclear envelope (Figure 5A) and upon exposure to air the arrested blastomeres continue to progress through mitosis, as seen by the formation of the metaphase plate and chromosome segregation (Figure 5B). Mitotic progression from prophase to anaphase is normal in *npp-16(ok1839)* embryos exposed to normoxia (Figure 5C, Video 5). However, the *npp-16(ok1839)* mutant embryos exposed to anoxia contained prophase blastomeres in which the chromosomes did not completely align with the nuclear periphery (8 of 26 prophase blastomeres) or NEBD occurred, as determined by the eventual loss of a circular nucleus, resulting in blastomeres with abnormal chromosome structure (8 of 26 prophase blastomeres analyzed; Figure 5D, Video 6). However, in some cases (10 of 26) prophase arrest, and chromosome alignment with the nuclear periphery occurred, indicating that the abnormal anoxia arrest phenotype is not 100% penetrant in the *npp-16(ok1839)* mutant. Together, these data further support the notion that, unlike control embryos, the prophase blastomeres from *npp-16(ok1839)* animals do not consistently arrest in response to anoxia, pointing to a novel important function of nucleoporins in oxygen-controlled cell cycle progression.

NPC distribution, as detected by the mAb414 mAb, was abnormal in some *npp-16(ok1839)* blastomeres of embryos exposed to anoxia (Figure 3, arrowhead). Therefore, we considered the possibility that the permeability of the nuclear envelope was compromised in *npp-16(ok1839)* embryos under these conditions. The permeability of the nuclear envelope can be monitored by using fluorescently labeled dextran molecules (Galy *et al.*, 2003; Lenart and Ellenberg, 2006); smaller molecules 20 kDa or below are able to diffuse through the NPC; however, if the NPC transport function is compromised, then larger macromolecules (70 kDa) will also pass into the nucleus (Galy *et al.*, 2003; Lenart and Ellenberg, 2006). To assay nuclear permeability of control and *npp-16(ok1839)* embryos exposed to either anoxia or normoxia, we used a fluorescently labeled 70-kDa dextran. To assay the nuclear permeability in the context of the respective cell cycle position, we used TH32 (control strain) and *npp-16(ok1839)* crossed into the TH32 background, which express GFP-tagged γ-tubulin and histone2B. The 70-kDa dextran was excluded from prophase and interphase nuclei of both control and *npp-16(ok1839)* embryos exposed to either anoxia or normoxia (Figure 6, Table S1). Notably, the 70-kDa dextran was also excluded from nuclei in the abnormal blastomeres of *npp-16(ok1839)* embryos exposed to anoxia (Figure 6, arrow), indicating that the permeability barrier through the NPC or nuclear envelope remained intact, despite the abnormal NPC distribution associated with *npp-16(ok1839)* embryos. To determine if the nucleus is more permeable to molecules smaller than 70 kDa, we conducted similar assays using the 40- and 10-kDa dextran molecules. The 40-kDa dextran molecule behaved similarly to the 70-kDa dextran molecule in that dextran was excluded from the prophase and interphase nuclei in both control and *npp-16(ok1839)* embryos exposed to normoxia or anoxia (data not shown). This data indicates that nucleus permeability was likely not severely compromised in these blastomeres. The

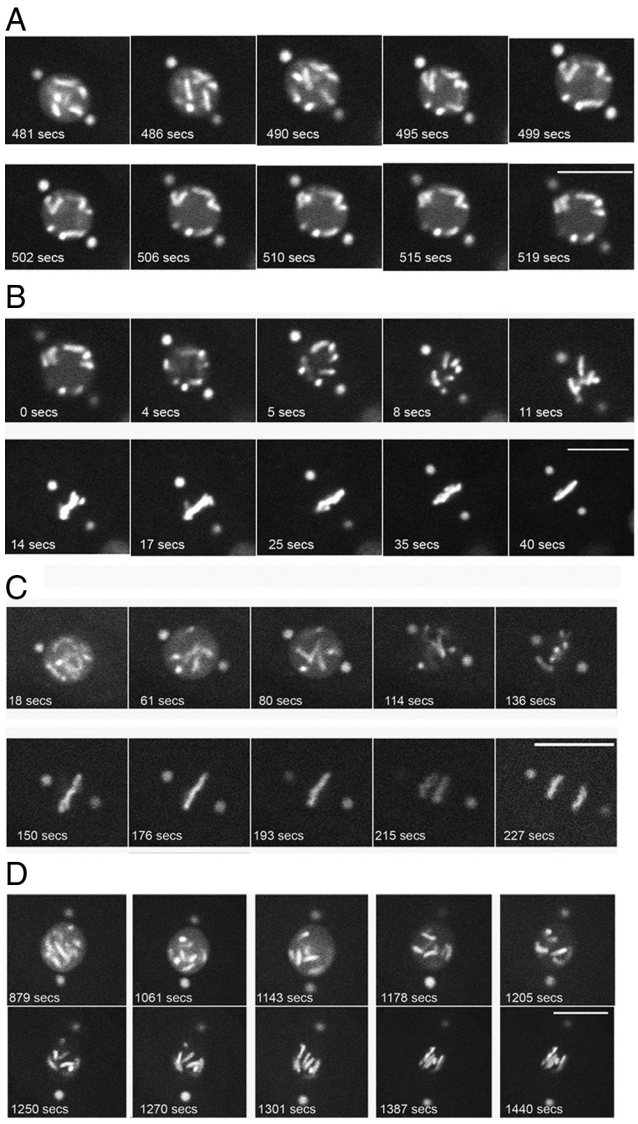

Figure 5. The arrested *npp-16(ok1839)* prophase blastomere is abnormal. Live cell imaging analysis, of control TH32 strain and *npp-16(ok1839)* crossed into the TH32 background, to visualize chromosome location and mitotic progression. Shown are representative images from a time-lapse microscopy experiment to assay the nuclei of prophase blastomeres in control embryos exposed to anoxia (A) or after anoxia (B) and nuclei of prophase blastomeres in *npp-16(ok1839)* embryos exposed to normoxia (C) or anoxia (D). For each data set, a total of at least 10 prophase blastomeres were examined. The N_2 gas flow-through chamber was used to expose animals to anoxia. Scale bar, 5 μm.

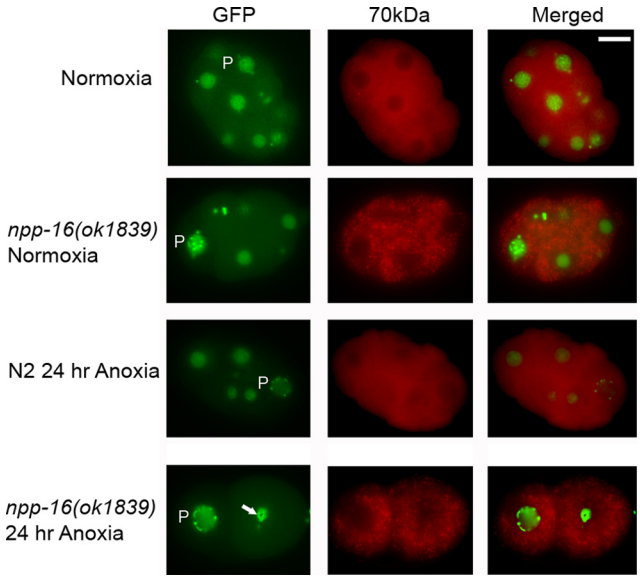

Figure 6. The permeability of the nuclear envelope in *npp-16(ok1839)* embryos is not completely compromised. The permeability of the nuclear envelope was monitored using fluorescently labeled dextran (TRITC-labeled 70-kDa dextran) in the context of cell cycle position (TH32 strain used) in control and *npp-16(ok1839)* embryos exposed to normoxia or 24 h of anoxia. The letter P is left of prophase a blastomere, and arrow points to a nuclei with abnormal chromosome structure. In these experiments at least 57 blastomeres from 16 or more embryos were analyzed (see Table S1). Scale bar, 10 μm.

10-kDa dextran molecule is small enough to diffuse into the nucleus, and we did observe diffusion of the 10-kDa dextran molecule in many, but not all, of the nuclei in both control and *npp-16(ok1839)* blastomeres exposed to anoxia or normoxia (Table S1). Note that in several cases we observed that the dextran molecules (70, 40, and 10 kDa) aggregated within the cytoplasm, which could contribute to the inability to diffuse into the nucleus. However given that the 70- or 40-kDa dextran molecules did not diffuse into the nucleus of *npp-16(ok1839)* blastomeres exposed to anoxia suggest that the requirement of *npp-16* function to arrest prophase blastomeres in response to anoxia is not merely due to abnormal nuclear transport of macromolecules.

To characterize the germ line phenotype in *npp-16(ok1839)* hermaphrodites, we used the TH32 strain backcrossed into the *npp-16(ok1839)* strain or stained the gonad, of *npp-16(ok1839)* hermaphrodites, with mAb414 and DAPI to recognize the NPC and chromosomes, respectively. We observed several phenotypes associated with the *npp-16(ok1839)* mutation. First, unlike control animals, the *npp-16(ok1839)* hermaphrodites exposed to normoxia contain oocytes in which the bivalent chromosomes associate with the inner nuclear periphery; this was observed in animals analyzed by live imaging analysis or by immunostaining of the gonad (Figure S3 and Table S2; Figure 7B). Analysis of the *npp-16(ok1839)* hermaphrodites exposed to anoxia indicates that many of the oocytes had an abnormal nucleus as determined by an abnormal shape or if the membrane, as detected by mAb414, was not round/oblong and appeared to have invaginations or folds (Table S2 and Figure S3; Figure 7B). We also observed phenotypes associated with anoxia exposure (Figure 7). Others have shown, in the wild-type germ line, that mAb414 localizes at cluster regions in germ cell nuclei (Pitt *et al.*, 2000). We observe in control germ cells mAb414 localized around the nuclear DNA. However, in both wild-type and *npp-16(ok1839)* animals the localization of mAb414 is more dispersed in the germ cells within the pachytene region of the gonad (Figure 7B), suggesting that the NPC of these germ cells are perturbed in response to anoxia. Second, in oocytes the mAb414 detection accumulates at the cortical region of the oocyte and is not as intense at the nucleus in comparison to normoxic controls (Figure 7A, cf. oocytes noted by asterisk and arrow). Third, the sperm are always visible in the gonad of anoxia-exposed animals (Figure 7A, region noted as SP); this suggests that ovulation may arrest in a specific manner, but further analysis of the spermatheca would need to be conducted to determine if such is the case.

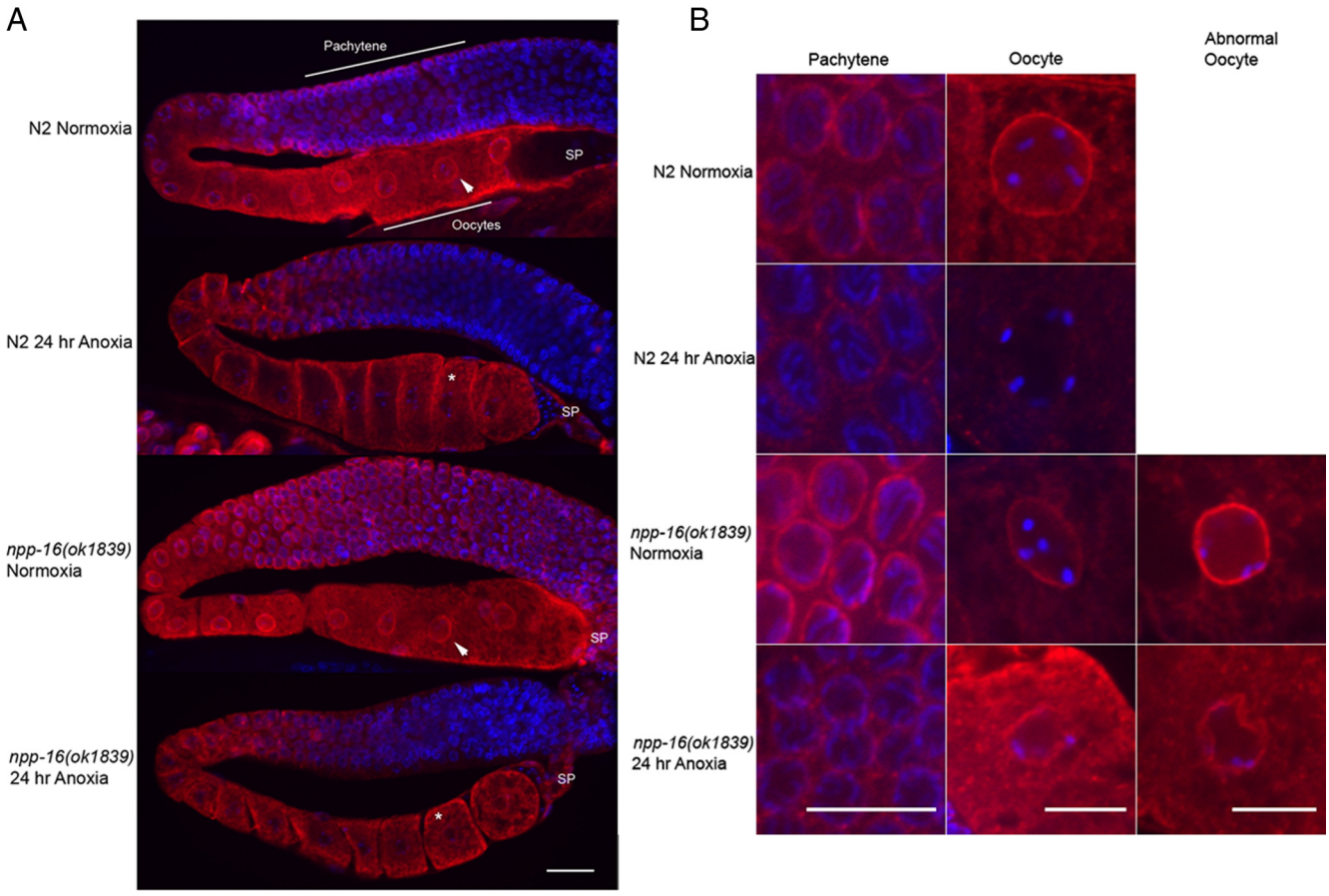

Figure 7. The germline of wild-type and *npp-16(ok139)* adult hermaphrodites exposed to normoxia or anoxia. Shown are representative images of N2 wild-type and *npp-16(ok1839)* adult gonads dissected and stained with DAPI to detect DNA and mAb414 to detect NPC. Either the entire gonad region is shown (A) or an enlarged image of the pachytene region, normal oocytes, or abnormal oocytes (B). In A the NPC is noted by an arrowhead, SP denotes the spermatheca region, and asterisk notes the observation that in anoxia-exposed animals the mAb414 detection accumulates at the cortical region of the oocyte. Note that in comparison to control, the anoxia-exposed animals the localization of mAb414 appears more dispersed within the pachytene region of the gonad (B). We classified oocytes as abnormal if the bivalent chromosomes associated with the nuclear periphery under normoxic conditions or if the nuclear membrane shape was not round/oblong and appeared to have invaginations or folds (B). Quantification of these phenotypes and the number of animals and oocytes analyzed are noted in Table S2. Scale bars, 10 μm.

Together, these results suggest that in the oocyte of animals exposed to anoxia, *npp-16* is not required for chromosome association with the nuclear periphery but is required for maintenance of nuclear shape. Furthermore, anoxia affects the localization of NPC in the meiotic cells of both wild-type and *npp-16(ok1839)* animals, further supporting the idea that the NPC has a role in anoxia responses. To determine if aged oocytes were viable in *npp-16(ok1839)* hermaphrodites depleted of sperm, as determined by the lack of offspring and occasional unfertilized oocyte on NGM plate, the hermaphrodites were mated with adult N2 males; 62.5% of the *npp-16(ok1839)* hermaphrodites (n = 16) were able to produce offspring in which a large frequency of males were observed. In comparison, 83% of sperm-depleted wild-type hermaphrodites produced offspring (n = 6). Together our data indicates that the gonad of *npp-16(ok1839)* animals is functional but has some phenotypes associated with the mutation.

Activity State of Cyclin-dependent Kinase (CDK-1) in Control and npp-16(ok1839) Prophase Blastomeres

Several nucleoporins are known to have transport-independent functions including a possible role in NEBD, kinetochore function, gene regulation, and chromosome segregation (D'Angelo and Hetzer, 2008; Capelson and Hetzer, 2009). To further test the hypothesis that prophase arrest is controlled genetically and that this control is compromised in *npp-16(ok1839)* embryos, we conducted a cell biological analysis to assay CDK-1 activity. In yeast and mammalian cells, a critical component for the commitment and progression through mitosis is activation of the Cdk1/cyclin B1 complex (Nurse, 1990; Margalit *et al.*, 2005). In our hands, the sterility observed in *cdk-1(RNAi)* hermaphrodites is near 100% (data not shown), and thus it is not straightforward to genetically determine if CDK-1 function is necessary for anoxia-induced prophase arrest in embryos (Burrows *et al.*, 2006). Therefore, we took a cell biological approach to investigate CDK-1 function in relation to prophase arrest. We used antiserum raised against the C-terminus of CDK-1 (anti-CDK-1) or a phospho-specific antibody (CDK-1$^{P\text{-}Tyr15}$) to detect the inactive form of CDK-1 (Figure 8). Others have shown, using the anti-CDK-1 antibody, that CDK-1 is localized to the nucleus and cytoplasm in *C. elegans* embryos (Boxem *et al.*, 1999). We found that in normoxic control and *npp-16(ok1839)* embryos (n = 58 and 42, respectively) the majority of prophase blastomeres contain CDK-1 localized to the cytoplasm and nucleus yet in some cases anti-CDK-1

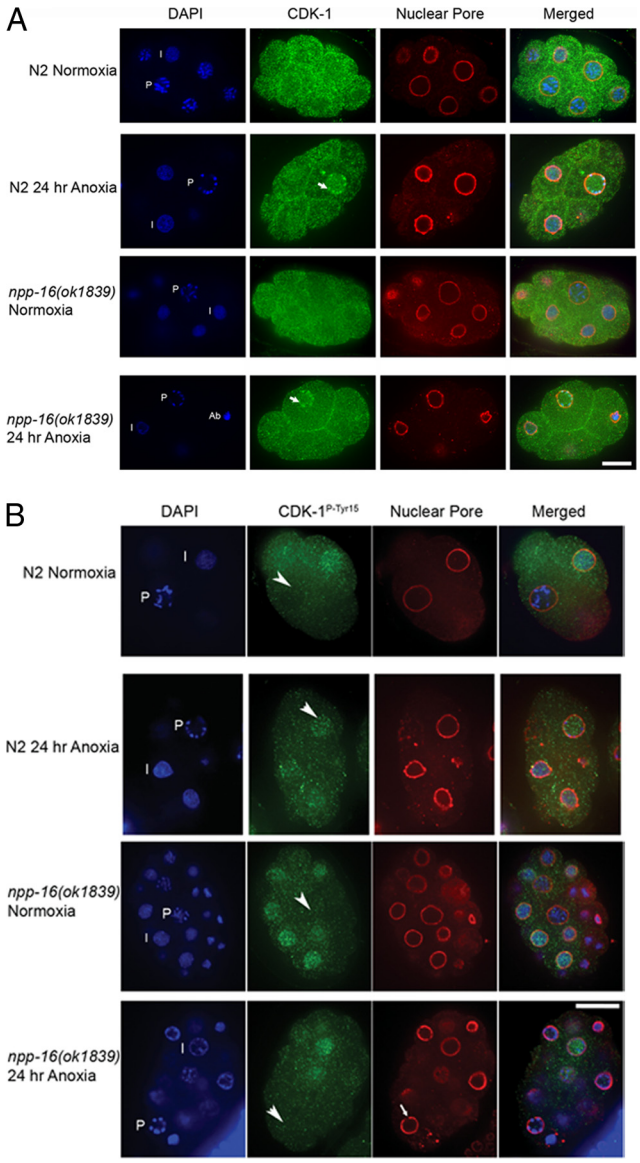

Figure 8. Activity state of cyclin-dependent kinase (CDK-1) differs in control and *npp-16(ok1839)* arrested prophase blastomeres. The *npp-16(ok1839)* and N2 wild-type embryos, exposed to either normoxia or anoxia, were stained with DAPI to detect DNA, mAb414 to detect NPC, and either anti-CDK-1 (A) or anti CDK-1$^{P\text{-}Tyr15}$ (B). Prophase blastomeres (P), interphase blastomeres (I), and abnormal nuclei (Ab) are denoted as such. (A) Arrow points to prophase blastomeres in which anti-CDK-1 is detected near the proximity of chromosomes associated with the inner nuclear periphery. (B) Arrowhead points to prophase blastomeres. Note the detection of inactive CDK-1 in the nucleus of arrested N2 prophase blastomeres but the absence in the nucleus of arrested *npp-16(ok1839)* prophase blastomeres. (B) The arrow points to a blastomere in which the distribution of NPC is discontinuous in the *npp-16(ok1839)* embryo exposed to anoxia. For each data set three independent experiments were conducted in which a final total of 100 blastomeres from at least 50 embryos were examined. Scale bar, 10 μm.

signal is brighter in the cytoplasm relative to the nucleus (21.6 and 5.9%, respectively) or brighter in the nucleus relative to the cytoplasm (10.8 and 23.5%, respectively). Interestingly, embryos exposed to anoxia contain prophase blastomeres in which CDK-1 is localized on or near the chromosomes associated with the inner nuclear periphery (Figure 8A arrow). In wild-type embryos exposed to anoxia the majority of prophase blastomeres (92.8%, n = 28) contained anti-CDK-1 localized with the chromosomes, whereas this was the case with ~50% (n = 10) of the *npp-16(ok1839)* prophase blastomeres of embryos exposed to anoxia. The anti-CDK-1 was detected on or near chromosomes within abnormal blastomeres of *npp-16(ok1839)* embryos exposed to anoxia (40%, n = 30). The association with chromosomes was not observed in embryos exposed to normoxia indicating that CDK-1 localization is altered in response to anoxia.

During interphase, Cdk1 is phosphorylated and in an inactive form, and its dephosphorylation during mitosis activates the complex and leads to Cdk1-catalyzed phosphorylation of inner nuclear membrane proteins which is required for NEBD in mammalian cells (Heald and McKeon, 1990; Margalit *et al.*, 2005). To determine the localization pattern of the inactive form of CDK-1 in *C. elegans* exposed to anoxia, we used the phospho-specific antibody (CDK-1$^{P\text{-}Tyr15}$) in wild-type and *npp-16(ok1839)* embryos (De Souza *et al.*, 2000; Hachet *et al.*, 2007). Similarly to what others have shown in the *C. elegans* zygote (Hachet *et al.*, 2007), inactive CDK-1$^{P\text{-}Tyr15}$ was detected in the nucleus of interphase blastomeres but was absent from the nuclei of late prophase blastomeres (Figure 8B), suggesting the presence of active CDK-1 in prophase blastomeres of wild-type N2 embryos (100%, n = 20; Figure 8B). We observed a similar pattern of CDK-1$^{P\text{-}Tyr15}$ in the *npp-16(ok1839)* embryos exposed to normoxia (100%, n = 18; Figure 8B); thus, deletion of *npp-16* did not result in abnormal regulation of CDK-1 in a normoxic environment. In wild-type embryos exposed to anoxia, however, CDK-1$^{P\text{-}Tyr15}$ was detected in the nuclei of arrested prophase blastomeres (81%, n = 26), indicating the presence of inactive CDK-1 (Figure 8B). The protein recognized by anti-CDK-1$^{P\text{-}Tyr15}$ is throughout the nucleus, and thus it is not clear whether the inactive form is also localized to the chromosomes in a similar manner as the CDK-1 detected by anti-CDK-1 (Figure 8B, arrowhead). Note that we do not observe identical overlap between the anti-CDK-1 and anti-CDK-1$^{P\text{-}Tyr15}$ in anoxic prophase blastomeres of wild-type embryos, suggesting that various isoforms of CDK-1 are located within the arrested prophase nucleus. In marked contrast to the wild-type arrested prophase blastomeres, CDK-1$^{P\text{-}Tyr15}$ was not detectable (79%, n = 29) in prophase blastomeres of *npp-16(ok1839)* embryos exposed to anoxia, suggesting that CDK-1 is in an active state in these blastomeres (Figure 8B, arrowhead). In these experiments we only assayed prophase blastomeres of embryos in which CDK-1$^{P\text{-}Tyr15}$ was detectable in interphase blastomeres to exclude the possibility that lack of CDK-1$^{P\text{-}Tyr15}$ detection was due to insufficient staining and to ensure that the antibody indeed entered into the embryo. Furthermore, we restricted the analysis to the few prophase blastomeres that are observed in *npp-16(ok1839)* embryos under anoxia conditions and excluded from the analysis nuclei with the abnormal morphology (as seen in Figure 3). These data show for the first time that CDK-1 localization and posttranslational modifications are altered in arrested prophase blastomeres and suggests that the activity state of CDK-1 plays a role in anoxia-induced prophase arrest and that CDK-1 activity is misregulated in the *npp-16(ok1839)* prophase blastomeres exposed to anoxia.

DISCUSSION

We conducted cellular and genetic analysis of prophase cells exposed to anoxia to gain a greater understanding of mechanisms regulating arrest of prophase cells. Using

time-lapse microscopy, we found that chromosomes associate with the inner nuclear periphery in anoxia-induced arrested prophase blastomeres. Others have shown that chromosomes associate with the nuclear periphery in *Drosophila* prophase cells exposed to anoxia (Foe and Alberts, 1985), indicating that this response to oxygen deprivation is conserved. We found that oocytes, of anoxia exposed adults, aged adults, or adults that have dysfunctional sperm (*fog-2(q71)* mutant), contain bivalent chromosomes associated with the nuclear periphery. However, we did not observe this in the oocytes of starved adults. Others have shown that brief, acute, and chronic starvation induces a variety of cellular and behavioral responses. However, the specific response to starvation often depends on the stage at which starvation was induced and how long the animals were exposed to starvation. Known germline responses to starvation include an increase in programmed cell death, arrest of germ cell proliferation, and reproductive diapause. Recently, it was shown that after 5 d of starvation L4 larvae will either arrest as L4 larvae, as adults with the germline in reproductive diapause or become adults in which embryos in the uterus develop and cause death of the adult due to vivipary (bagging out; Angelo and Van Gilst, 2009). In our experiment we found that many of the adults were holding embryos in the uterus after 12 h without a food source, and longer periods of starvation led to the bagging out phenotype (data not shown), indicating that the lack of food was indeed inducing a physiological response. However, it may be of interest to determine if a specific starvation regimen does induce chromosome association with the inner nuclear periphery in the oocyte. Embryos and oocytes exposed to the electron transport inhibitor sodium azide contain nuclei with chromosomes associated with the nuclear periphery. However, unlike anoxia exposure, blastomeres exposed for longer periods to sodium azide led to abnormal nuclei suggesting that anoxia-induced arrest is likely not just due to inhibition of electron transport activity. Together, these results demonstrate that chromosome association with the nuclear periphery occurs in both mitotic and meiotic cells and may be a characteristic of arrested or quiescent cells rather than stressed cells.

The relevance of chromosome association with the nuclear periphery, in anoxia-exposed blastomeres or oocytes, is not understood. Many studies have shown that in interphase cells, transcriptional regulation and silencing of genes is associated with the localization of chromatin to the nuclear periphery (Shaklai *et al.,* 2007). In *Drosophila* and yeast it has been shown that chromosomal loci at the nuclear periphery interact with nuclear pores and that nuclear pores can interact with both transcriptionally inactive and active loci (Casolari *et al.,* 2004; Akhtar and Gasser, 2007). Several nucleoporins as well as nucleoporin-associated proteins (MLP1, MLP2) are required for full repression of specific loci, indicating that NPC has a role in gene regulation (Galy *et al.,* 2000; Feuerbach *et al.,* 2002). An alternative reason for prophase chromosome association with the inner nuclear periphery, in arrested cells, may be to maintain genome stability. It has been shown that stabilization of repetitive DNA sequences (rDNA repeats), which are prone to homologous recombination, occurs by interactions between inner nuclear membrane proteins and chromosomal proteins (Mekhail *et al.,* 2008). In anoxia-arrested prophase cells and oocytes the chromosomes are highly condensed and thus likely to not be transcriptionally active. Furthermore, we found that the quiescent oocytes in the sperm-dysfunctional *fog-2* mutant or sperm-depleted aged hermaphrodite also contain oocytes with bivalent chromosomes associated with the inner nuclear periphery; these quiescent oocytes are viable and have other phenotypes similar to that of oocytes exposed to anoxia (Jud *et al.,* 2008). We suggest that the relevance of chromosome association with the nuclear periphery in these arrested cells may not be to regulate gene expression but rather to maintain genome stability and/or chromosome structure in times of arrest. Thus, it may be possible that the mechanisms for maintaining oocytes in an arrested or quiescent state are overlapping, regardless if the arrest is induced by anoxia exposure, inhibition of electron transport activity, sperm depletion, or sperm dysfunction. It will be of interest to determine if anoxia-induced chromosome association with the nuclear periphery is important for genome stability and if this phenomenon is an essential component for arresting prophase cells.

The NPC is a large protein channel associated with the nuclear envelope and made up of nucleoporins. This highly conserved protein structure is important for the transport of macromolecules between the cytoplasm and nucleoplasm. Recently, there is increasing evidence that the nucleoporins are involved with a variety of cellular processes including chromatin organization, gene regulation, and spindle orientation (Schetter *et al.,* 2006; Capelson and Hetzer, 2009). Furthermore, it has been shown that some nucleoporins (Nup107) not only localize to the NPC but, upon NPC disassembly, relocalize to chromatin during mitosis (Galy *et al.,* 2006). Phenotypic analysis of the *npp-16(ok1839)* embryo exposed to anoxia indicates that *npp-16* is required for prophase arrest. This is supported by the finding that there is a decrease in arrested prophase blastomeres and an increase in abnormal prophase blastomeres in *npp-16(ok1839)* embryos exposed to anoxia. Analysis of the *npp-16(ok1839)* oocytes suggests that *npp-16* is also required for maintenance of oocytes. This is supported by the finding that *npp-16(ok1839)* hermaphrodites exposed to normal air conditions contain bivalent chromosomes associated with the nuclear periphery. The *npp-16(ok1839)* hermaphrodites exposed to anoxia have oocytes with chromosomes associated with the nuclear periphery, yet many of these oocytes have an abnormally shaped nucleus. These results suggest that in the oocyte *npp-16* is not required for chromosome association with the nuclear periphery but is required for maintenance of nuclear shape in oocytes of animals exposed to anoxia.

Using a fluorescently labeled dextran molecule, we show that the permeability of the *npp-16(ok1839)* embryo exposed to normoxia or anoxia does not appear abnormal (Figure 6). This indicates that the nuclear abnormalities observed in *npp-16(ok1839)* embryos exposed to anoxia may be due to cellular defects other than those affecting nuclear transport. The *C. elegans* NPP-16 has homology to the mammalian Nup50. The relative location of Nup50 is peripheral and at the nucleoplasm side of the NPC. Other than a role in nuclear transport, additional functions involving Nup50 are not known. However, using a two-hybrid analysis NUP50 was shown to interact with $p27^{kip1}$, a CDK/cyclin inhibitor, suggesting a role of NUP50 with cell cycle checkpoints (Sherr and Roberts, 1999; Smitherman *et al.,* 2000).

We used antibodies to detect CDK-1 and the phospho-specific antibody ($CDK\text{-}1^{P\text{-}Tyr15}$) to detect the inactive form of CDK-1 in wild-type and *npp-16(ok1839)* embryos exposed to normoxia or anoxia (Hachet *et al.,* 2007). Interestingly, we found that anti-CDK-1 was detected on or near chromosomes of prophase blastomeres exposed to anoxia. The relevance and activation state of CDK-1 associated with/near chromosomes in anoxic prophase blastomeres is not understood. Others have shown, using mammalian cell culture,

that cyclin B1 localizes to chromatin, centrosomes and kinetochore during mitosis yet localization of cyclin B1 to chromatin is independent of CDK1 binding (Bentley *et al.*, 2007). It will be of interest to determine if other cell cycle–regulated proteins are localized to chromatin in arrested prophase blastomeres. The lack of CDK-1$^{P\text{-}Tyr15}$ detection in prophase blastomeres indicates that the active form is present; this is the case for late prophase blastomeres of developing wild-type and *npp-16(ok1839)* embryos. Yet, the inactive form of CDK-1 (CDK-1$^{P\text{-}Tyr15}$) was detected in the arrested prophase blastomeres of wild-type embryos exposed to anoxia. Therefore, a potential mechanism to arrest prophase blastomeres in response to anoxia likely involves the inactivation of CDK-1. This model is possible given that CDK-1 is known to regulate the phosphorylation of several inner nuclear membrane proteins before NEBD (Heald and McKeon, 1990; Margalit *et al.*, 2005). Interestingly, the nucleus of prophase blastomeres of *npp-16(ok1839)* embryos exposed to anoxia contained the active form of CDK-1 (CDK-1$^{P\text{-}Tyr15}$ was not detected in). Thus, it is plausible that in anoxia-exposed *npp-16(ok1839)* prophase blastomeres the activated CDK-1 promotes NEBD, and thus the cells are unable to maintain prophase arrest. This interpretation is further supported by our finding that there is a decrease in the number of arrested prophase blastomeres in *npp-16(ok1839)* embryos exposed to anoxia. However, further studies will need to determine if the active form of CDK-1 in prophase blastomeres of *npp-16(ok1839)* embryos exposed to anoxia is the cause or the consequence of the abnormalities observed in the nuclei of these embryos. Additional studies are needed to elucidate the detailed mechanistic relationship between NPP-16 function and CDK-1 regulation in the context of anoxia-induced prophase arrest. In conclusion, our results support the idea that a natural stressor such as oxygen deprivation, regulates cell cycle arrest and that the nucleoporin NPP-16 and cell cycle regulator CDK-1 may have a role in a previously uncharacterized prophase checkpoint in the *C. elegans* embryo.

ACKNOWLEDGMENTS

We especially thank Dr. Sepp Kohlwein for helpful and insightful comments on the manuscript. We thank members of the Padilla lab and the UNT DPGR group for insightful discussions regarding this research and the *Caenorhabditis elegans* Genetics Stock Center, the Oklahoma Knockout Consortium, and Dr. Askjaer for strains. We acknowledge and thank Dr. Lon Turnbull for technical assistance with confocal microscopy, and Dr. Landon Moore (University of Southern Indiana), Dr. Golden, and Dr. Schumacher for antibodies. This work was supported by Grant R01-GM069419 from the National Institutes of Health, National Institute of General Medical Sciences to P.A.P.

REFERENCES

Akhtar, A., and Gasser, S. M. (2007). The nuclear envelope and transcriptional control. Nat. Rev. Genet *8*, 507–517.

Anderson, D. J., and Hetzer, M. W. (2008). The life cycle of the metazoan nuclear envelope. Curr. Opin. Cell Biol. *20*, 386–392.

Angelo, G., and Van Gilst, M. R. (2009). Starvation protects germline stem cells and extends reproductive longevity in *C. elegans.* Science. *326*, 954–958.

Beaudouin, J., Gerlich, D., Daigle, N., Eils, R., and Ellenberg, J. (2002). Nuclear envelope breakdown proceeds by microtubule-induced tearing of the lamina. Cell *108*, 83–96.

Bentley, A. M., Normand, G., Hoyt, J., and King, R. W. (2007). Distinct sequence elements of cyclin B1 promote localization to chromatin, centrosomes, and kinetochores during mitosis. Mol. Biol. Cell *18*, 4847–4858.

Boxem, M., Srinivasan, D. G., and van den Heuvel, S. (1999). The *Caenorhabditis elegans* gene ncc-1 encodes a cdc2-related kinase required for M phase in meiotic and mitotic cell divisions, but not for S phase. Development *126*, 2227–2239.

Buchwitz, B. J., Ahmad, K., Moore, L. L., Roth, M. B., and Henikoff, S. (1999). A histone-H3-like protein in *C. elegans.* Nature *401*, 547–548.

Burrows, A. E., Sceurman, B. K., Kosinski, M. E., Richie, C. T., Sadler, P. L., Schumacher, J. M., and Golden, A. (2006). The *C. elegans* Myt1 ortholog is required for the proper timing of oocyte maturation. Development *133*, 697–709.

Cahill, D. P., Lengauer, C., Yu, J., Riggins, G. J., Willson, J. K., Markowitz, S. D., Kinzler, K. W., and Vogelstein, B. (1998). Mutations of mitotic checkpoint genes in human cancers. Nature *392*, 300–303.

Capelson, M., and Hetzer, M. W. (2009). The role of nuclear pores in gene regulation, development and disease. EMBO Rep. *10*, 697–705.

Casolari, J. M., Brown, C. R., Komili, S., West, J., Hieronymus, H., and Silver, P. A. (2004). Genome-wide localization of the nuclear transport machinery couples transcriptional status and nuclear organization. Cell *117*, 427–439.

D'Angelo, M. A., and Hetzer, M. W. (2008). Structure, dynamics and function of nuclear pore complexes. Trends Cell Biol. *18*, 456–466.

De Souza, C. P., Ellem, K. A., and Gabrielli, B. G. (2000). Centrosomal and cytoplasmic Cdc2/cyclin B1 activation precedes nuclear mitotic events. Exp. Cell Res. *257*, 11–21.

DiGregorio, P. J., Ubersax, J. A., and O'Farrell, P. H. (2001). Hypoxia and nitric oxide induce a rapid, reversible cell cycle arrest of the *Drosophila* syncytial divisions. J. Biol. Chem. *276*, 1930–1937.

Douglas, R. M., Xu, T., and Haddad, G. G. (2001). Cell cycle progression and cell division are sensitive to hypoxia in *Drosophila melanogaster* embryos. Am J. Physiol. Regul. Integr. Comp. Physiol. *280*, R1555–R1563.

Encalada, S. E., Willis, J., Lyczak, R., and Bowerman, B. (2005). A spindle checkpoint functions during mitosis in the early *Caenorhabditis elegans* embryo. Mol. Biol. Cell *16*, 1056–1070.

Feuerbach, F., Galy, V., Trelles-Sticken, E., Fromont-Racine, M., Jacquier, A., Gilson, E., Olivo-Marin, J. C., Scherthan, H., and Nehrbass, U. (2002). Nuclear architecture and spatial positioning help establish transcriptional states of telomeres in yeast. Nat. Cell Biol. *4*, 214–221.

Fischer, M. G., Heeger, S., Hacker, U., and Lehner, C. F. (2004). The mitotic arrest in response to hypoxia and of polar bodies during early embryogenesis requires *Drosophila* Mps1. Curr. Biol. *14*, 2019–2024.

Foe, V. E., and Alberts, B. M. (1985). Reversible chromosome condensation induced in *Drosophila* embryos by anoxia: visualization of interphase nuclear organization. J. Cell Biol. *100*, 1623–1636.

Galy, V., Antonin, W., Jaedicke, A., Sachse, M., Santarella, R., Haselmann, U., and Mattaj, I. (2008). A role for gp210 in mitotic nuclear-envelope breakdown. J. Cell Sci. *121*, 317–328.

Galy, V., Askjaer, P., Franz, C., Lopez-Iglesias, C., and Mattaj, I. W. (2006). MEL-28, a novel nuclear-envelope and kinetochore protein essential for zygotic nuclear-envelope assembly in *C. elegans.* Curr. Biol. *16*, 1748–1756.

Galy, V., Mattaj, I. W., and Askjaer, P. (2003). Caenorhabditis elegans nucleoporins Nup93 and Nup205 determine the limit of nuclear pore complex size exclusion in vivo. Mol. Biol. Cell *14*, 5104–5115.

Galy, V., Olivo-Marin, J. C., Scherthan, H., Doye, V., Rascalou, N., and Nehrbass, U. (2000). Nuclear pore complexes in the organization of silent telomeric chromatin. Nature *403*, 108–112.

Green, S. L., Freiberg, R. A., and Giaccia, A. J. (2001). p21(Cip1) and p27(Kip1) regulate cell cycle reentry after hypoxic stress but are not necessary for hypoxia-induced arrest. Mol. Cell. Biol. *21*, 1196–1206.

Hachet, V., Canard, C., and Gonczy, P. (2007). Centrosomes promote timely mitotic entry in *C. elegans* embryos. Dev. Cell *12*, 531–541.

Hajeri, V. A., Stewart, A. M., Moore, L. L., and Padilla, P. A. (2008). Genetic analysis of the spindle checkpoint genes san-1, mdf-2, bub-3 and the CENP-F homologues hcp-1 and hcp-2 in *Caenorhabditis elegans.* Cell Div. *3*, 6.

Hajeri, V. A., Trejo, J., and Padilla, P. A. (2005). Characterization of sub-nuclear changes in *Caenorhabditis elegans* embryos exposed to brief, intermediate and long-term anoxia to analyze anoxia-induced cell cycle arrest. BMC Cell Biol. *6*, 47.

Hardwick, K. G., Li, R., Mistrot, C., Chen, R. H., Dann, P., Rudner, A., and Murray, A. W. (1999). Lesions in many different spindle components activate the spindle checkpoint in the budding yeast *Saccharomyces cerevisiae.* Genetics *152*, 509–518.

Hartwell, L. H., and Weinert, T. A. (1989). Checkpoints: controls that ensure the order of cell cycle events. Science *246*, 629–634.

Heald, R., and McKeon, F. (1990). Mutations of phosphorylation sites in lamin A that prevent nuclear lamina disassembly in mitosis. Cell *61*, 579–589.

Jud, M. C., *et al.* (2008). Large P body-like RNPs form in *C. elegans* oocytes in response to arrested ovulation, heat shock, osmotic stress, and anoxia and are regulated by the major sperm protein pathway. Dev. Biol. *318*, 38–51.

Kamath, R. S., *et al.* (2003). Systematic functional analysis of the *Caenorhabditis elegans* genome using RNAi. Nature *421*, 231–237.

Kiseleva, E., Rutherford, S., Cotter, L. M., Allen, T. D., and Goldberg, M. W. (2001). Steps of nuclear pore complex disassembly and reassembly during mitosis in early *Drosophila* embryos. J. Cell Sci. *114*, 3607–3618.

Lee, K. K., Gruenbaum, Y., Spann, P., Liu, J., and Wilson, K. L. (2000). *C. elegans* nuclear envelope proteins emerin, MAN1, lamin, and nucleoporins reveal unique timing of nuclear envelope breakdown during mitosis. Mol. Biol. Cell *11*, 3089–3099.

Lenart, P., and Ellenberg, J. (2006). Monitoring the permeability of the nuclear envelope during the cell cycle. Methods *38*, 17–24.

Lenart, P., Rabut, G., Daigle, N., Hand, A. R., Terasaki, M., and Ellenberg, J. (2003). Nuclear envelope breakdown in starfish oocytes proceeds by partial NPC disassembly followed by a rapidly spreading fenestration of nuclear membranes. J. Cell Biol. *160*, 1055–1068.

Margalit, A., Vlcek, S., Gruenbaum, Y., and Foisner, R. (2005). Breaking and making of the nuclear envelope. J. Cell. Biochem. *95*, 454–465.

McCarter, J., Bartlett, B., Dang, T., and Schedl, T. (1999). On the control of oocyte meiotic maturation and ovulation in *Caenorhabditis elegans*. Dev. Biol. *205*, 111–128.

Mekhail, K., Seebacher, J., Gygi, S. P., and Moazed, D. (2008). Role for perinuclear chromosome tethering in maintenance of genome stability. Nature *456*, 667–670.

Mendenhall, A. R., LeBlanc, M. G., Mohan, D. P., and Padilla, P. A. (2009). Reduction in ovulation or male sex phenotype increases long-term anoxia survival in a daf-16-independent manner in *Caenorhabditis elegans*. Physiol. Genomics *36*, 167–178.

Moore, L. L., Morrison, M., and Roth, M. B. (1999). HCP-1, a protein involved in chromosome segregation, is localized to the centromere of mitotic chromosomes in *Caenorhabditis elegans*. J. Cell Biol. *147*, 471–480.

Nurse, P. (1990). Universal control mechanism regulating onset of M-phase. Nature *344*, 503–508.

Nurse, P., Masui, Y., and Hartwell, L. (1998). Understanding the cell cycle. Nat. Med. *4*, 1103–1106.

Nystul, T. G., Goldmark, J. P., Padilla, P. A., and Roth, M. B. (2003). Suspended animation in *C. elegans* requires the spindle checkpoint. Science *302*, 1038–1041.

Oegema, K., Desai, A., Rybina, S., Kirkham, M., and Hyman, A. A. (2001). Functional analysis of kinetochore assembly in *Caenorhabditis elegans*. J. Cell Biol. *153*, 1209–1226.

Padilla, P. A., Nystul, T. G., Zager, R. A., Johnson, A. C., and Roth, M. B. (2002). Dephosphorylation of cell cycle-regulated proteins correlates with anoxia-induced suspended animation in *Caenorhabditis elegans*. Mol. Biol. Cell *13*, 1473–1483.

Padilla, P. A., and Roth, M. B. (2001). Oxygen deprivation causes suspended animation in the zebrafish embryo. Proc. Natl. Acad. Sci. USA *98*, 7331–7335.

Pandey, R., Heeger, S., and Lehner, C. F. (2007). Rapid effects of acute anoxia on spindle kinetochore interactions activate the mitotic spindle checkpoint. J. Cell Sci. *120*, 2807–2818.

Pitt, J. N., Schisa, J. A., and Priess, J. R. (2000). P granules in the germ cells of *Caenorhabditis elegans* adults are associated with clusters of nuclear pores and contain RNA. Dev. Biol. *219*, 315–333.

Reis, R. M., Nakamura, M., Masuoka, J., Watanabe, T., Colella, S., Yonekawa, Y., Kleihues, P., and Ohgaki, H. (2001). Mutation analysis of hBUB1, hBUBR1 and hBUB3 genes in glioblastomas. Acta Neuropathol. *101*, 297–304.

Rodenas, E., Klerkx, E. P., Ayuso, C., Audhya, A., and Askjaer, P. (2009). Early embryonic requirement for nucleoporin Nup35/NPP-19 in nuclear assembly. Dev. Biol. *327*, 399–409.

Salina, D., Bodoor, K., Eckley, D. M., Schroer, T. A., Rattner, J. B., and Burke, B. (2002). Cytoplasmic dynein as a facilitator of nuclear envelope breakdown. Cell *108*, 97–107.

Schedl, T., and Kimble, J. (1988). fog-2, a germ-line-specific sex determination gene required for hermaphrodite spermatogenesis in *Caenorhabditis elegans*. Genetics *119*, 43–61.

Schetter, A., Askjaer, P., Piano, F., Mattaj, I., and Kemphues, K. (2006). Nucleoporins NPP-1, NPP-3, NPP-4, NPP-11 and NPP-13 are required for proper spindle orientation in *C. elegans*. Dev. Biol. *289*, 360–371.

Shaklai, S., Amariglio, N., Rechavi, G., and Simon, A. J. (2007). Gene silencing at the nuclear periphery. FEBS J. *274*, 1383–1392.

Sherr, C. J., and Roberts, J. M. (1999). CDK inhibitors: positive and negative regulators of G1-phase progression. Genes Dev. *13*, 1501–1512.

Smitherman, M., Lee, K., Swanger, J., Kapur, R., and Clurman, B. E. (2000). Characterization and targeted disruption of murine Nup50, a p27(Kip1)-interacting component of the nuclear pore complex. Mol. Cell. Biol. *20*, 5631–5642.

Sulston, J. E., and Hodgkin, J. (1988). Methods. In: The Nematode *Caenorhabditis elegans*. Cold Spring Harbor, NY: Cold Spring Harbor Laboratory Press. 587–606.